# On the construction of PML absorbing boundary condition for the non-linear Euler equations

Fang. Q. Hu\*

Department of Mathematics and Statistics, Old Dominion University Norfolk, Virginia 23529

A Perfectly Matched Layer (PML) absorbing boundary condition for the nonlinear Euler equations in two space dimensions is presented. The derivation of PML equation follows athree-step method recently developed for the PML of linearized Euler equations. Two versions of time-domain PML equations are given. One uses unsplit physical variables and the other uses the split equation in the derivation but requires fewer auxiliary variables. Both versions are given for the nonlinear Euler equation written in the conservation form, so they can be implemented easily in most existing codes. To increase the efficiency of the PML, a pseudo mean-flow is introduced in the derivation of the PML equations. The proposed PML absorbs exponentially the difference between the nonlinear total variable and a prescribed pseudo mean flow. Moreover, the non-linear PML reduces to the linearized PML upon linearization about the pseudo mean-flow. The validity and efficiency of PML as an absorbing boundary condition for non-linear Euler equations are demonstrated by numerical examples, including the absorption of an isentropic vortex, a nonlinear pressure pulse and roll-up vortices of shear flows. Satisfactory computational results are reported.

#### I. Introduction

Non-reflecting boundary condition is a critical component in the development of Computational Aeroacoustics (CAA) algorithms. It remains a significant challenge particularly for problems involving non-linear or non-constant coefficient governing equations. Perfectly Matched Layer (PML) is a technique of developing non-reflecting boundary conditions by constructing modified governing equations that can absorb out-going waves at open computational boundaries. It was originally designed for computational electromagnetics. <sup>2</sup>, <sup>3</sup>, <sup>5</sup>, <sup>16</sup>, <sup>17</sup> The significance of the PML technique lies in the fact that the absorbing zone is theoretically reflectionless for multi-dimensional linear waves of any angle and frequency. Substantial progress has been made in the past few years on the development of the PML technique for the Euler equations, starting with the studies for constant mean-flows, followed by their extensions to cases with non-uniform mean-flows. <sup>1</sup>, <sup>6-8</sup>, <sup>10-12</sup>, <sup>14</sup> Most recently, applications of PML to linearized Navier-Stokes equations and even nonlinear Navier-Stokes equations have been discussed in [8].

One emerging theory of formulating PML absorbing boundary conditions for the governing equations of fluid dynamics involves essentially three steps. <sup>12,14</sup> First, a proper space-time transformation is determined and applied to the governing equations to ensure consistency of phase and group velocities of the linear waves; second, the transformed equation is modified with a PML complex change of variable in the frequency domain; and finally, the time domain absorbing boundary condition is derived. This three-step process has been applied recently for linearized Euler equations and produced highly accurate and numerically stable absorbing boundary conditions. <sup>12,14</sup>

<sup>\*</sup>Professor, Senior member AIAA

Copyright © 2006 by F. Q. Hu. Published by the American Institute of Aeronautics and Astronautics, Inc., with permission.

In this paper, the PML for the fully non-linear Euler equations is constructed following the three steps outlined above. In our derivation, the non-linear Euler equations are written in the conservation form, so the PML equations can be readily and easily implemented in most existing codes. To absorb the non-linear disturbances, the concept of "pseudo mean-flow" is introduced. This makes the PML possible without knowing the exact mean-flow which is often not available before the computation. Linearization at the boundary is not required. The boundary condition absorbs exponentially the difference between the pseudo mean-flow and the non-linear disturbances including the vorticity, acoustic and entropy waves. After the derivation, numerical examples that validate the effectiveness and stability of the PML for nonlinear Euler equations will be presented. They include the absorption of non-linear shear layer roll-up vortices, and a convective isentropic vortex in a compressible flow.

In the next section, time-domain PML for the non-linear Euler equation is derived. Further discussions on the suitable pseudo mean-flow are given in section III. Numerical examples are presented in section IV. Section V has the concluding remarks.

## II. Formulation

We consider the two-dimensional nonlinear Euler equation written in the conservation form,

$$\frac{\partial \mathbf{u}}{\partial t} + \frac{\partial \mathbf{F}_1(\mathbf{u})}{\partial x} + \frac{\partial \mathbf{F}_2(\mathbf{u})}{\partial y} = 0 \tag{1}$$

where

$$\mathbf{u} = \begin{bmatrix} \rho \\ \rho u \\ \rho v \\ \rho e \end{bmatrix}, \quad \mathbf{F}_1 = \begin{bmatrix} \rho u \\ \rho u^2 + p \\ \rho u v \\ \rho h u \end{bmatrix}, \quad \mathbf{F}_2 = \begin{bmatrix} \rho v \\ \rho u v \\ \rho v^2 + p \\ \rho h v \end{bmatrix}$$
 (2)

and

$$h = e + \frac{p}{\rho}, \ p = (\gamma - 1)\rho\left(e - \frac{u^2 + v^2}{2}\right)$$
 (3)

In (2) and (3), u and v are the velocity components, p is the pressure,  $\rho$  is the density and e is the energy. Specific heats ratio  $\gamma = 1.4$ .

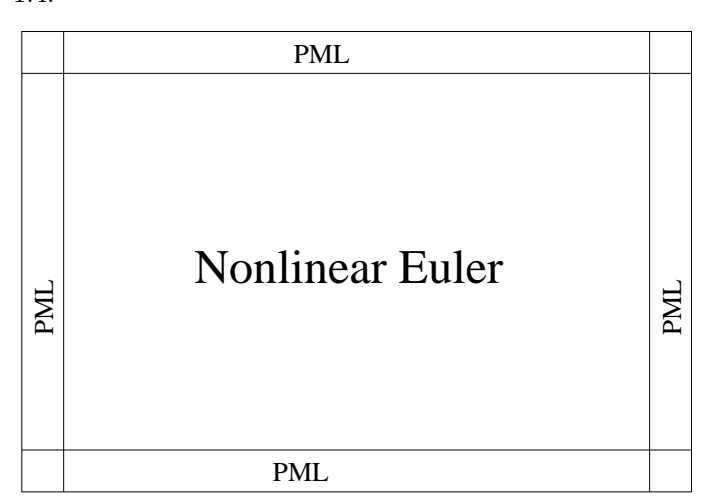


Figure 1. Schematic of Euler and PML domains with four open boundaries.

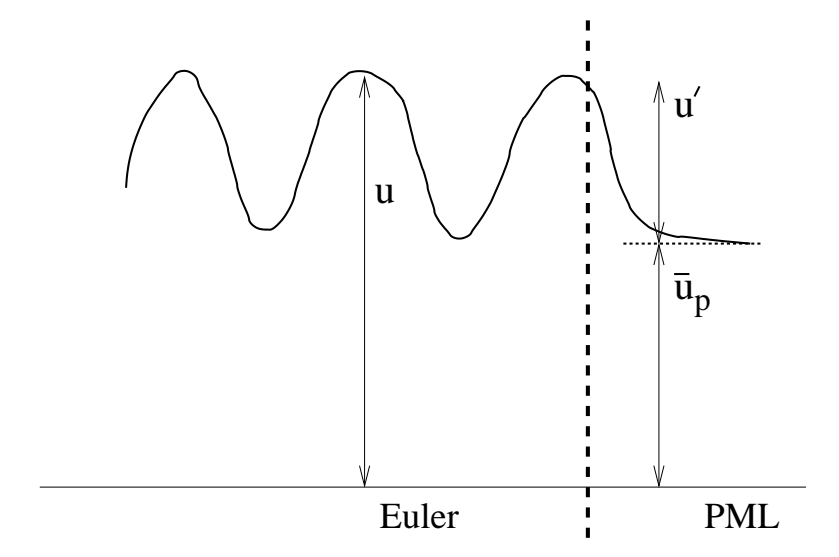


Figure 2. Absorption of nonlinear disturbances with a pseudo mean-flow in the PML domain.

At non-reflecting boundaries, we introduce PML domains to absorb out-going disturbances, as shown in Figure 1. We wish to formulate equations to be applied in the PML domain so that the disturbances can be exponentially reduced once they enter the added zones. At the same time, the use of PML equations should cause little or no reflection at the interface of the Euler and PML domains. By reducing the disturbances to a negligible level, the use of PML makes a non-reflecting boundary condition unnecessary at outer boundaries of the whole computational domain.

Since the total variable **u** could be quite large in a non-linear simulation, it may not be most efficient to absorb **u** and to reduce it to nearly zero inside the PML domain. Although it is common to decompose the total variable **u** into a time-independent mean-flow and a time-dependent fluctuation, the exact mean state is usually unknown at the start of the computation. The PML formulation presented here will not require the exact mean-flow. Instead, we shall partition the solution inside the PML domain into two parts as

$$\mathbf{u} = \bar{\mathbf{u}}_p + \mathbf{u}' \tag{4}$$

where  $\bar{\mathbf{u}}_p$  is a time-independent "pseudo mean-flow<sup>11</sup>". It is important to note that it is not necessary for this pseudo mean-flow to be the exact mean-flow at the non-reflecting boundary. The only requirement for  $\bar{\mathbf{u}}_p$  is that it satisfies the steady Euler equation:

$$\frac{\partial \mathbf{F}_1(\bar{\mathbf{u}}_p)}{\partial x} + \frac{\partial \mathbf{F}_2(\bar{\mathbf{u}}_p)}{\partial y} = 0 \tag{5}$$

The use of  $\bar{\mathbf{u}}_p$  is strictly to make the PML domain more efficient since we now need only to absorb  $\mathbf{u}'$ , the difference between  $\mathbf{u}$  and a prescribed pseudo mean-flow  $\bar{\mathbf{u}}_p$ , as shown in Figure 2. Obviously, the choice for  $\bar{\mathbf{u}}_p$  is not unique. Further considerations on the construction of the pseudo mean-flow will be given later.

In what follows, we will develop PML equation that absorbs  $\mathbf{u}'$ , the difference between  $\mathbf{u}$  and  $\bar{\mathbf{u}}_p$  inside the PML domain. By equation (5), it is easy to see that the equation for  $\mathbf{u}'$  can be written as

$$\frac{\partial \mathbf{u}'}{\partial t} + \frac{\partial [\mathbf{F}_1(\mathbf{u}) - \mathbf{F}_1(\bar{\mathbf{u}}_p)]}{\partial x} + \frac{\partial [\mathbf{F}_2(\mathbf{u}) - \mathbf{F}_2(\bar{\mathbf{u}}_p)]}{\partial y} = 0$$
 (6)

To derive a stable PML absorbing boundary condition for (6), it is necessary to introduce a proper space-time transformation before applying the PML complex change of variable to (6), as stated in the introduction. The purpose of the transformation is to correct the dispersion relations of the linear waves supported by (6) such that all the linear waves have consistent phase and group velocities. To this end, we will apply a space-time transformation of the form

$$\bar{t} = t + \beta x \tag{7}$$

to equation (6) where  $\beta$  is a parameter based on the pseudo mean-flow employed, as suggested in [14]. More details on parameter  $\beta$  will be given in the next section. The transformation gives the following changes in partial differential derivatives, with respect to t and x, as

$$\frac{\partial}{\partial t} \to \frac{\partial}{\partial \bar{t}}, \quad \frac{\partial}{\partial x} \to \frac{\partial}{\partial x} + \beta \frac{\partial}{\partial \bar{t}}$$
 (8)

and (6) now becomes

$$\frac{\partial \mathbf{u}'}{\partial \bar{t}} + \beta \frac{\partial [\mathbf{F}_1(\mathbf{u}) - \mathbf{F}_1(\bar{\mathbf{u}}_p)]}{\partial \bar{t}} + \frac{\partial [\mathbf{F}_1(\mathbf{u}) - \mathbf{F}_1(\bar{\mathbf{u}}_p)]}{\partial x} + \frac{\partial [\mathbf{F}_2(\mathbf{u}) - \mathbf{F}_2(\bar{\mathbf{u}}_p)]}{\partial y} = 0$$
(9)

In the frequency domain, the above is

$$(-i\omega)(\tilde{\mathbf{u}}' + \beta[\mathbf{F}_1(\mathbf{u}) - \mathbf{F}_1(\bar{\mathbf{u}}_p)]) + \frac{\partial[\mathbf{F}_1(\mathbf{u}) - \mathbf{F}_1(\bar{\mathbf{u}}_p)]}{\partial x} + \frac{\partial[\mathbf{F}_2(\mathbf{u}) - \mathbf{F}_2(\bar{\mathbf{u}}_p)]}{\partial u} = 0$$
(10)

where a tilde denotes the time Fourier transformed quantity. Now we introduce the PML complex change of variables,

$$x \to x + \frac{i}{\omega} \int_{x_0}^x \sigma_x dx, \quad y \to y + \frac{i}{\omega} \int_{y_0}^y \sigma_y dy$$
 (11)

which results in changes in partial derivatives as

$$\frac{\partial}{\partial x} \to \frac{1}{1 + i \frac{\sigma_x}{\omega}} \frac{\partial}{\partial x}, \quad \frac{\partial}{\partial y} \to \frac{1}{1 + i \frac{\sigma_y}{\omega}} \frac{\partial}{\partial y}$$
 (12)

Further details on the absorption coefficients  $\sigma_x$  and  $\sigma_y$  are referred to [12, 14]. Under (11), equation (10) is modified to be

$$(-i\omega)(\tilde{\mathbf{u}}' + \beta[\mathbf{F}_1(\mathbf{u}) - \mathbf{F}_1(\bar{\mathbf{u}}_p)]) + \frac{1}{1 + i\frac{\sigma_x}{\omega}} \frac{\partial[\mathbf{F}_1(\mathbf{u}) - \mathbf{F}_1(\bar{\mathbf{u}}_p)]}{\partial x} + \frac{1}{1 + i\frac{\sigma_y}{\omega}} \frac{\partial[\mathbf{F}_2(\mathbf{u}) - \mathbf{F}_2(\bar{\mathbf{u}}_p)]}{\partial y} = 0$$
(13)

Equation (13) is the PML equation for (6) in the frequency domain. To write (13) in the time domain, we will present two approaches. The first uses unsplit physical variables while the second uses split equations but introduces fewer auxiliary variables.

### A. Unsplit version

In the unsplit approach, following [12, 14], we multiply  $(1 + i \frac{\sigma_x}{\omega})(1 + i \frac{\sigma_y}{\omega})$  to equation (13) and get

$$(-i\omega + \sigma_x + \sigma_y + i\frac{\sigma_x\sigma_y}{\omega})(\tilde{\mathbf{u}}' + \beta[\mathbf{F}_1(\mathbf{u}) - \mathbf{F}_1(\bar{\mathbf{u}}_p)]) + (1 + i\frac{\sigma_y}{\omega})\frac{\partial[\mathbf{F}_1(\mathbf{u}) - \mathbf{F}_1(\bar{\mathbf{u}}_p)]}{\partial x} + (1 + i\frac{\sigma_x}{\omega})\frac{\partial[\mathbf{F}_2(\mathbf{u}) - \mathbf{F}_2(\bar{\mathbf{u}}_p)]}{\partial y} = 0$$
(14)

By defining auxiliary variables  $\mathbf{q}$ ,  $\mathbf{q}_1$  and  $\mathbf{q}_2$  as

$$\frac{\partial \mathbf{q}}{\partial t} = \mathbf{u}',\tag{15}$$

$$\frac{\partial \mathbf{q}_1}{\partial t} = \mathbf{F}_1(\mathbf{u}) - \mathbf{F}_1(\bar{\mathbf{u}}_p),\tag{16}$$

$$\frac{\partial \mathbf{q}_2}{\partial t} = \mathbf{F}_2(\mathbf{u}) - \mathbf{F}_2(\bar{\mathbf{u}}_p),\tag{17}$$

the time domain equation for (14) can now be written as

$$\frac{\partial \mathbf{u}'}{\partial \bar{t}} + \beta \frac{\partial [\mathbf{F}_{1}(\mathbf{u}) - \mathbf{F}_{1}(\bar{\mathbf{u}}_{p})]}{\partial \bar{t}} + (\sigma_{x} + \sigma_{y})\mathbf{u}' + (\sigma_{x} + \sigma_{y})\beta[\mathbf{F}_{1}(\mathbf{u}) - \mathbf{F}_{1}(\bar{\mathbf{u}}_{p})] + \sigma_{x}\sigma_{y}\mathbf{q} + \sigma_{x}\sigma_{y}\beta\mathbf{q}_{1}$$

$$+ \frac{\partial [\mathbf{F}_{1}(\mathbf{u}) - \mathbf{F}_{1}(\bar{\mathbf{u}}_{p})]}{\partial x} + \frac{\partial [\mathbf{F}_{2}(\mathbf{u}) - \mathbf{F}_{2}(\bar{\mathbf{u}}_{p})]}{\partial y} + \sigma_{y}\frac{\partial \mathbf{q}_{1}}{\partial x} + \sigma_{x}\frac{\partial \mathbf{q}_{2}}{\partial y} = 0 \tag{18}$$

Finally, in the original space and time variables x and t, we get

$$\frac{\partial \mathbf{u}'}{\partial t} + \frac{\partial [\mathbf{F}_1(\mathbf{u}) - \mathbf{F}_1(\bar{\mathbf{u}}_p)]}{\partial x} + \frac{\partial [\mathbf{F}_2(\mathbf{u}) - \mathbf{F}_2(\bar{\mathbf{u}}_p)]}{\partial y} + \sigma_y \frac{\partial \mathbf{q}_1}{\partial x} + \sigma_x \frac{\partial \mathbf{q}_2}{\partial y} + (\sigma_x + \sigma_y)\mathbf{u}' + \sigma_x \beta [\mathbf{F}_1(\mathbf{u}) - \mathbf{F}_1(\bar{\mathbf{u}}_p)] + \sigma_x \sigma_y \mathbf{q} + \sigma_x \sigma_y \beta \mathbf{q}_1 = 0$$

Since the pseudo mean-flow is time-independent and satisfies the steady Euler equation, we have the following PML equation written in the original total variable  $\mathbf{u}$ ,

$$\frac{\partial \mathbf{u}}{\partial t} + \frac{\partial \mathbf{F}_{1}(\mathbf{u})}{\partial x} + \frac{\partial \mathbf{F}_{2}(\mathbf{u})}{\partial y} + \sigma_{y} \frac{\partial \mathbf{q}_{1}}{\partial x} + \sigma_{x} \frac{\partial \mathbf{q}_{2}}{\partial y} + (\sigma_{x} + \sigma_{y})(\mathbf{u} - \bar{\mathbf{u}}_{p}) + \sigma_{x}\beta[\mathbf{F}_{1}(\mathbf{u}) - \mathbf{F}_{1}(\bar{\mathbf{u}}_{p})] + \sigma_{x}\sigma_{y}\mathbf{q} + \sigma_{x}\sigma_{y}\beta\mathbf{q}_{1} = 0$$
(19)

Equations (19) and (15)-(17) are to be solved in the PML domain.

Before presenting a different way of deriving the time-domain equation, we note that, first, upon linearization about  $\bar{\mathbf{u}}_p$ , the above can be shown to be equivalent to the PML for the linearized Euler equations with a non-uniform mean-flow given in [14]. Second, there are three auxiliary variables introduced in the PML domain, which could increase computational storage and cost. For this reason, we next consider a split approach in forming the PML equation in which only one set of auxiliary variable is necessary.

## B. Split version

In the split approach, we rewrite the frequency domain PML (13) in two equations as follows, similar to what was done in the original PML formulation by Berenger,<sup>2</sup>

$$(-i\omega)(\tilde{\mathbf{u}}_1' + \beta[\mathbf{F}_1(\mathbf{u}) - \mathbf{F}_1(\bar{\mathbf{u}}_p)]) + \frac{1}{1 + i\frac{\sigma_x}{\omega}} \frac{\partial [\mathbf{F}_1(\mathbf{u}) - \mathbf{F}_1(\bar{\mathbf{u}}_p)]}{\partial x} = 0$$
 (20)

$$(-i\omega)\tilde{\mathbf{u}}_{2}' + \frac{1}{1 + i\frac{\sigma_{y}}{\omega}} \frac{\partial [\mathbf{F}_{2}(\mathbf{u}) - \mathbf{F}_{2}(\bar{\mathbf{u}}_{p})]}{\partial y} = 0$$
(21)

where we have

$$\mathbf{u}' = \mathbf{u}_1' + \mathbf{u}_2' \tag{22}$$

As we can see, by adding the two equations (20) and (21), we will recover (13). To write the above in the time domain, we multiply  $(1+i\frac{\sigma_x}{\omega})$  and  $(1+i\frac{\sigma_y}{\omega})$  to (20) and (21), respectively, and get

$$(-i\omega + \sigma_x)(\tilde{\mathbf{u}}_1' + \beta[\mathbf{F}_1(\mathbf{u}) - \mathbf{F}_1(\bar{\mathbf{u}}_p)]) + \frac{\partial[\mathbf{F}_1(\mathbf{u}) - \mathbf{F}_1(\bar{\mathbf{u}}_p)]}{\partial x} = 0$$

$$(-i\omega + \sigma_y)\tilde{\mathbf{u}}_2' + \frac{\partial [\mathbf{F}_2(\mathbf{u}) - \mathbf{F}_2(\bar{\mathbf{u}}_p)]}{\partial y} = 0$$

which yields immediately

$$(-i\omega)(\tilde{\mathbf{u}}_{1}' + \beta[\mathbf{F}_{1}(\mathbf{u}) - \mathbf{F}_{1}(\bar{\mathbf{u}}_{p})]) + \sigma_{x}(\tilde{\mathbf{u}}_{1}' + \beta[\mathbf{F}_{1}(\mathbf{u}) - \mathbf{F}_{1}(\bar{\mathbf{u}}_{p})]) + \frac{\partial[\mathbf{F}_{1}(\mathbf{u}) - \mathbf{F}_{1}(\bar{\mathbf{u}}_{p})]}{\partial x} = 0$$

$$(-i\omega)\tilde{\mathbf{u}}_{2}' + \sigma_{y}\tilde{\mathbf{u}}_{2}' + \frac{\partial [\mathbf{F}_{2}(\mathbf{u}) - \mathbf{F}_{2}(\bar{\mathbf{u}}_{p})]}{\partial y} = 0$$

The above can be written easily in the time domain as

$$\frac{\partial \mathbf{u}_{1}'}{\partial \bar{t}} + \beta \frac{\partial [\mathbf{F}_{1}(\mathbf{u}) - \mathbf{F}_{1}(\bar{\mathbf{u}}_{p})]}{\partial \bar{t}} + \sigma_{x}(\mathbf{u}_{1}' + \beta [\mathbf{F}_{1}(\mathbf{u}) - \mathbf{F}_{1}(\bar{\mathbf{u}}_{p})]) + \frac{\partial [\mathbf{F}_{1}(\mathbf{u}) - \mathbf{F}_{1}(\bar{\mathbf{u}}_{p})]}{\partial x} = 0$$

$$\frac{\partial \mathbf{u}_2'}{\partial \bar{t}} + \sigma_y \mathbf{u}_2' + \frac{\partial [\mathbf{F}_2(\mathbf{u}) - \mathbf{F}_2(\bar{\mathbf{u}}_p)]}{\partial y} = 0$$

Finally, in the original space and time variables x and t, we get

$$\frac{\partial \mathbf{u}_{1}'}{\partial t} + \sigma_{x}\mathbf{u}_{1}' + \sigma_{x}\beta[\mathbf{F}_{1}(\mathbf{u}) - \mathbf{F}_{1}(\bar{\mathbf{u}}_{p})] + \frac{\partial[\mathbf{F}_{1}(\mathbf{u}) - \mathbf{F}_{1}(\bar{\mathbf{u}}_{p})]}{\partial x} = 0$$
(23)

$$\frac{\partial \mathbf{u}_2'}{\partial t} + \sigma_y \mathbf{u}_2' + \frac{\partial [\mathbf{F}_2(\mathbf{u}) - \mathbf{F}_2(\bar{\mathbf{u}}_p)]}{\partial y} = 0$$
(24)

These two equations form the PML for absorbing  $\mathbf{u}'$  in the PML domain.

We can also rewrite these two equations slightly differently for implementational convenience, as was done in some previous PML works.<sup>9,15</sup> By adding (24) to (23) and replacing  $\mathbf{u}_1'$  with  $\mathbf{u}' - \mathbf{u}_2'$ , (23) may be written alternatively as

$$\frac{\partial \mathbf{u}'}{\partial t} + \sigma_x(\mathbf{u}' - \mathbf{u}_2') + \sigma_y \mathbf{u}_2' + \sigma_x \beta [\mathbf{F}_1(\mathbf{u}) - \mathbf{F}_1(\bar{\mathbf{u}}_p)] + \frac{\partial [\mathbf{F}_1(\mathbf{u}) - \mathbf{F}_1(\bar{\mathbf{u}}_p)]}{\partial x} + \frac{\partial [\mathbf{F}_2(\mathbf{u}) - \mathbf{F}_2(\bar{\mathbf{u}}_p)]}{\partial y} = 0$$

Finally, by renaming  $\mathbf{u}_2'$  the auxiliary variable  $\mathbf{q}$  and noting the fact that  $\bar{\mathbf{u}}_p$  is independent of time and satisfies the steady Euler equation, we have the following equations to be used in PML domains,

$$\frac{\partial \mathbf{u}}{\partial t} + \frac{\partial \mathbf{F}_1(\mathbf{u})}{\partial x} + \frac{\partial \mathbf{F}_2(\mathbf{u})}{\partial y} + \sigma_x(\mathbf{u} - \bar{\mathbf{u}}_p - \mathbf{q}) + \sigma_y\mathbf{q} + \sigma_x\beta[\mathbf{F}_1(\mathbf{u}) - \mathbf{F}_1(\bar{\mathbf{u}}_p)] = 0$$
 (25)

$$\frac{\partial \mathbf{q}}{\partial t} + \sigma_y \mathbf{q} + \frac{\partial [\mathbf{F}_2(\mathbf{u}) - \mathbf{F}_2(\bar{\mathbf{u}}_p)]}{\partial y} = 0$$
 (26)

In this way, only one auxiliary variable,  $\mathbf{q}$ , is necessary.

# III. Pseudo mean-flow and value for $\beta$

In our derivations above, the only requirement on the pseudo mean-flow  $\bar{\mathbf{u}}_p$  is that it satisfy the steady state Euler equation (5). It is not necessary and, most of the time, not possible, for  $\bar{\mathbf{u}}_p$  to be the exact mean-flow. Thus, the choice of pseudo mean-flow is not unique. Any known solution to the steady Euler equation (5) that resembles the actual flow can be a good candidate for the pseudo mean-flow in the formulation of the PML equation. In many practical problems, such a pseudo mean-flow is relatively easy to find. In fact, any parallel flow will satisfy the steady state Euler equation and thus can be used as a pseudo mean-flow for the appropriate non-linear flows. For instance, in primitive variables,

$$\left[\begin{array}{c} \rho \\ u \\ v \\ p \end{array}\right] = \left[\begin{array}{c} \bar{\rho}_p(y) \\ \bar{u}_p(y) \\ 0 \\ \bar{p}_p \end{array}\right]$$

will satisfy (5) where  $\bar{\rho}_p(y)$  and  $\bar{u}_p(y)$  can be arbitrarily adjusted to resemble the flow at the boundary.

Once the pseudo mean-flow is chosen, the parameter  $\beta$  in the PML equation is determined as described in [14]. The purpose of the space-time transformation given in (7) is to ensure linear stability of the PML equation. More details are referred to [14]. Since the PML equations derived in this paper reduce to that for the linearized Euler equation given in [14], the value for  $\beta$  can be found in the same way as that presented in [14], based on the pseudo mean-flow employed. In general, a study on the dispersion relation  $D(\omega, k)$  for the linear waves supported by the pseudo mean-flow is necessary to determine the value of  $\beta$ . For a special case where the density of the pseudo mean-flow is constant, i.e.,  $\bar{\rho}_p(y) = 1$ , we may use a simple empirical formula given in [14],

$$\beta = \frac{\bar{U}_m}{1 - \bar{U}_m^2}, \ \bar{U}_m = \frac{1}{b - a} \int_a^b \bar{u}_p(y) dy$$

where the computational domain for y is [a, b].

# IV. Numerical examples

In this section, we present numerical examples that verifies the effectiveness of the PML derived in this paper for the non-linear Euler equation. Both the unsplit and split versions of PML given in section II have been tested computationally with no discernible differences in the results obtained. All the computations reported here use the split version (25)-(26) in the PML domain.

# A. Isentropic vortex

The non-linear Euler equation supports advective solution of the form

$$\begin{pmatrix} \rho(\mathbf{x},t) \\ u(\mathbf{x},t) \\ v(\mathbf{x},t) \\ p(\mathbf{x},t) \end{pmatrix} = \begin{pmatrix} 0 \\ U_0 \\ V_0 \\ 0 \end{pmatrix} + \begin{pmatrix} \rho_r(r) \\ -u_r(r)\sin\theta \\ u_r(r)\cos\theta \\ p_r(r) \end{pmatrix}$$
(27)

where  $r = \sqrt{(x - U_0 t)^2 + (y - V_0 t)^2}$  and, for any given  $u_r(r)$  and  $\rho_r(r)$ , the pressure  $p_r(r)$  is found by

$$\frac{d}{dr}p_r(r) = \rho_r(r)\frac{u_r^2(r)}{r} \tag{28}$$

Equation (27) gives a solution that advects with constant velocity  $(U_0, V_0)$ .

For our numerical tests, we consider a velocity distribution of the form

$$u_r(r) = \frac{U'_{max}}{b} r e^{\frac{1}{2}(1 - \frac{r^2}{b^2})}$$
 (29)

where  $U'_{max}$  is the maximum velocity at r = b. For isentropic flow, we assume

$$p_r = \frac{1}{\gamma} \rho_r^{\gamma} \tag{30}$$

and, by integrating (28), we get the following density and pressure distributions,

$$\rho_r(r) = \left(1 - \frac{1}{2}(\gamma - 1)U_{max}^{\prime 2}e^{1 - \frac{r^2}{b^2}}\right)^{1/(\gamma - 1)}$$
(31)

$$p_r(r) = \frac{1}{\gamma} \left( 1 - \frac{1}{2} (\gamma - 1) U_{max}^{\prime 2} e^{1 - \frac{r^2}{b^2}} \right)^{\gamma/(\gamma - 1)}$$
(32)

A numerical solution is shown in Figure 3. The initial condition is that given in (27) with  $(U_0, V_0) = (0.5, 0)$  and  $U'_{max} = 0.25$  and b = 0.3. The non-linear Euler equation (1) is solved by a finite difference scheme. The computational domain is  $[-1.2, 1.2] \times [-1.2, 1.2]$  with  $\Delta x = \Delta y = 0.02$ , including the surrounding PML domain of width 10 grid points. Further details on the numerics can be found in [14]. In particular, the PML absorption coefficient

$$\sigma_x = \sigma_{max} \left| \frac{x - x_0}{D} \right|^{\alpha}$$

with  $\sigma_{max} = 20$ ,  $\alpha = 4$  and similar model for  $\sigma_y$  is used. A grid stretching in the PML domain is also used to increase the efficiency of the absorbing zone.<sup>17</sup> The stretch factor is

$$\alpha(x) = 1 + 2 \left| \frac{x - x_0}{D} \right|^2$$

as noted in [14].

Figures 3(a)-(d) show the v-velocity contours at time t = 0, 1.5, 2.5 and 3.5 respectively, at levels from  $\pm 0.02$  to  $\pm 0.4$ . Absorption of vortex by PML at the outflow boundary is clearly demonstrated. Figure 4 shows the v-velocity as a function of x along y = 0, as the vortex exits the computational domain. Also plotted in dashed lines are the exact solution. As we can see, the numerical solution matches the exact solution in the Euler domain while decays exponentially in the PML domain.

To further assess the reflection error, Figure 5 plots the maximum difference between the numerical solution and a reference solution obtained using a larger computational domain, along a vertical line near the outflow boundary, as a function of time. The reflection errors are indeed quite small and reduces with an increase in the width of the PML domain employed.

Figure 6 shows the maximum reflection error relative to the maximum velocity of the vortex along x = 0.9 near the outflow boundary for various strengths of the vortex. Although reflection error generally increases with an increase in the strength of the vortex, a relative error of less than 1% is achieved for all cases with PML width of 20 grid points.

#### B. Pressure pulse

In the second example, we carry out a computation of the non-linear Euler equation with a strong pressure wave. The computation is initialized by

$$\rho = 1$$
,  $u = 0.5$ ,  $v = 0$ ,  $p = \frac{1}{\gamma} + A_0 e^{-\ln(2)(x^2 + y^2)/0.2^2}$ 

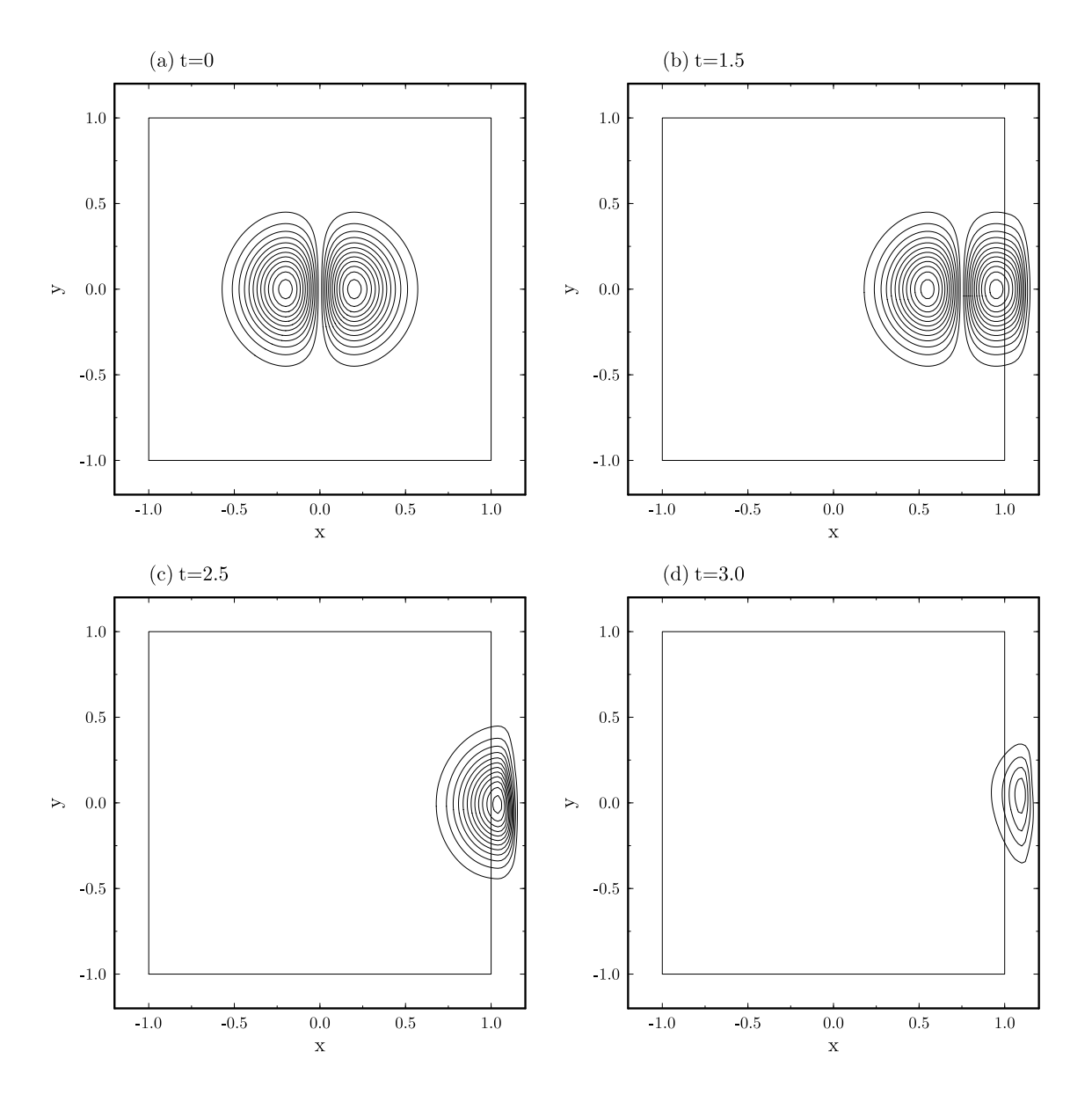


Figure 3. v-velocity contour levels from  $\pm 0.02$  to  $\pm 0.24$ .

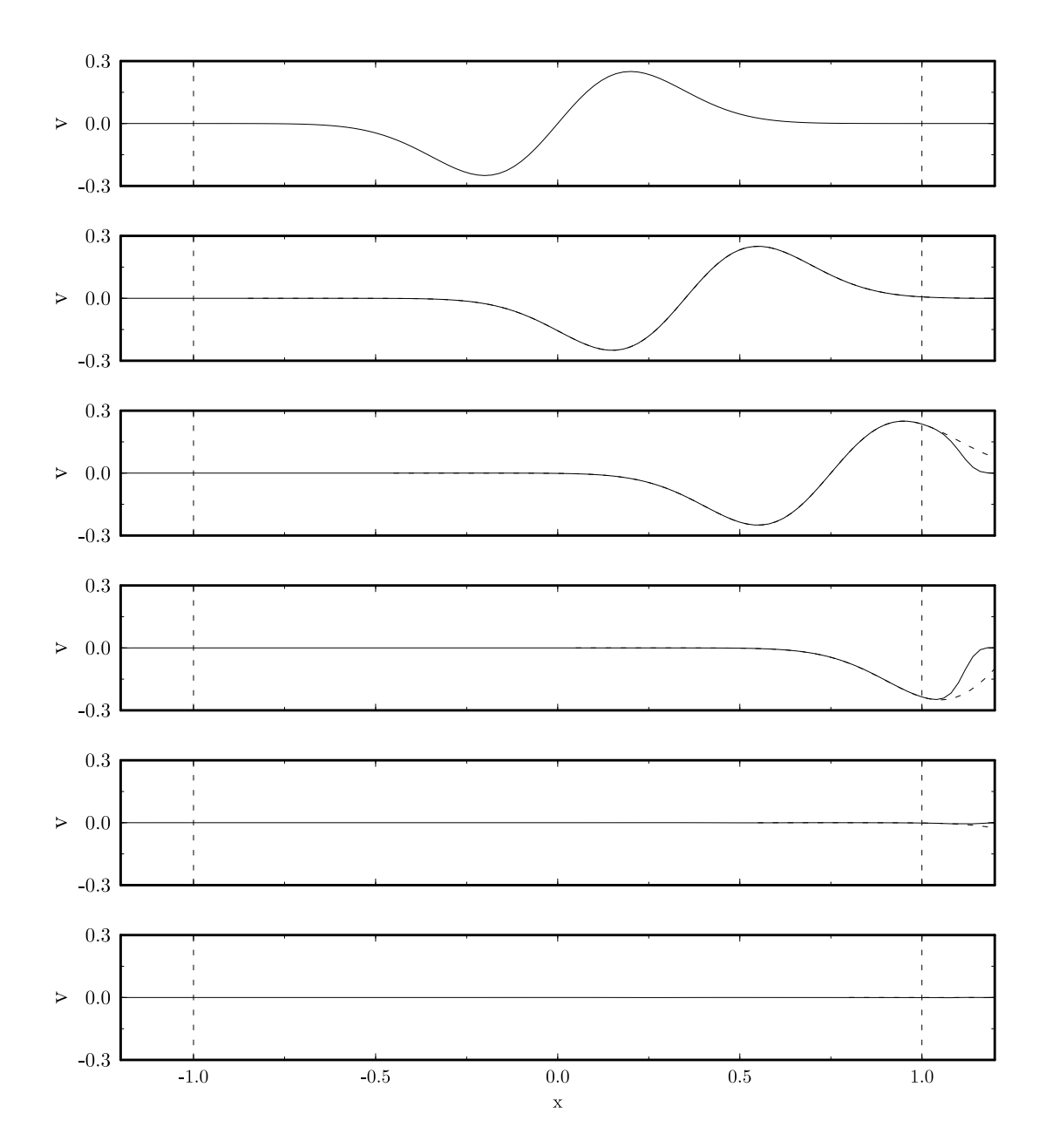


Figure 4. v-velocity profile along y=0 at progressive time frames. Solid line: numerical solution; dashed line: exact solution. Vertical dashed lines indicate the Euler/PML interface.

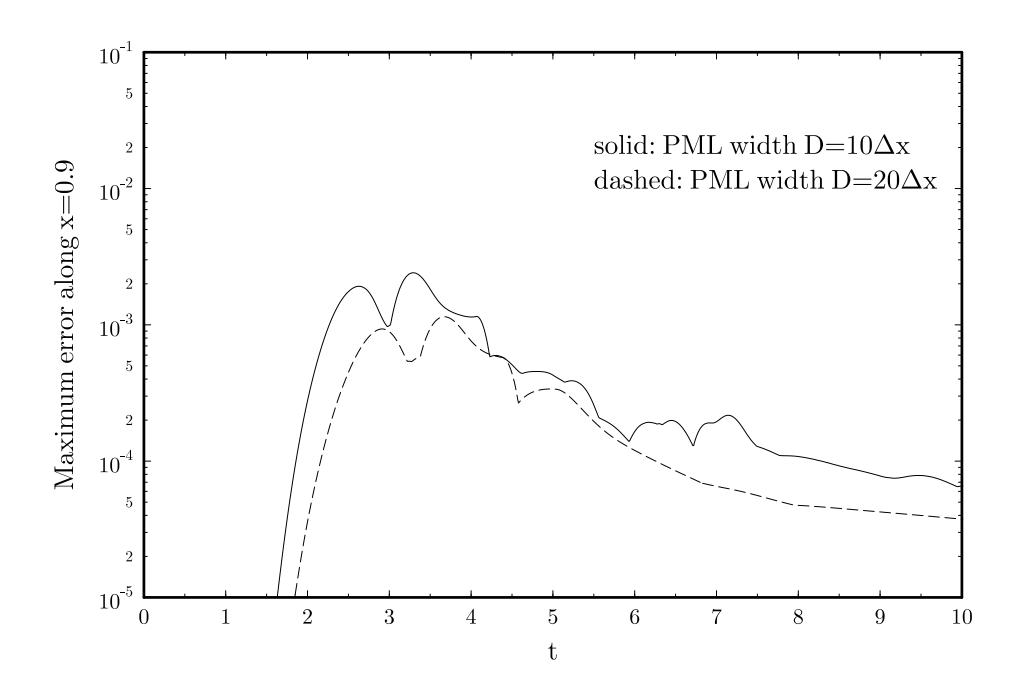


Figure 5. Maximum reflection error (v-velocity component) along x=0.9 near the outflow boundary. PML width is as indicated.

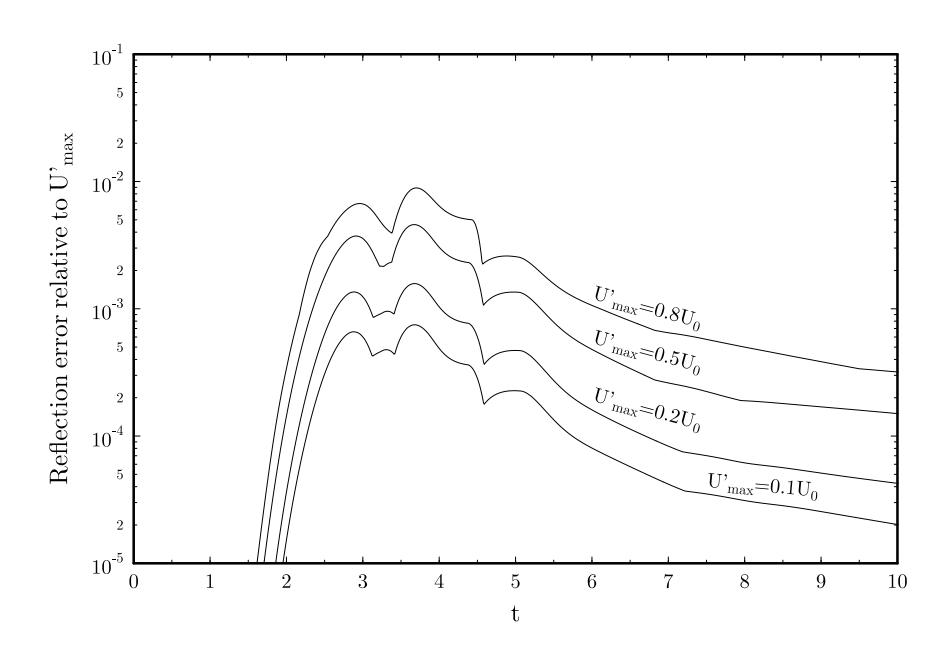


Figure 6. Maximum reflection error (v-velocity component) along x=0.9 near the outflow boundary. PML width  $D=20\Delta x$ .

where  $A_0 = 1$ . Figure 7 shows the pressure contours at time t = 0, 0.5, 1.0 and 1.5. Absorption of the non-linear pressure wave with little reflection is clearly demonstrated. Figure 8 shows the pressure profile as a function of x along y = 0. The strong pressure wave is obviously in the nonlinear regime and its absorption by the PML caused very little reflection.

In both examples shown above, the pseudo mean-flow  $\bar{\mathbf{u}}_p$  is the background uniform flow, i.e.,  $u = U_0 = 0.5$ ,  $v = V_0 = 0$ ,  $\rho = 1$  and  $p = 1/\gamma$ . The value of  $\beta$  is  $U_0/(1 - U_0^2)$ .

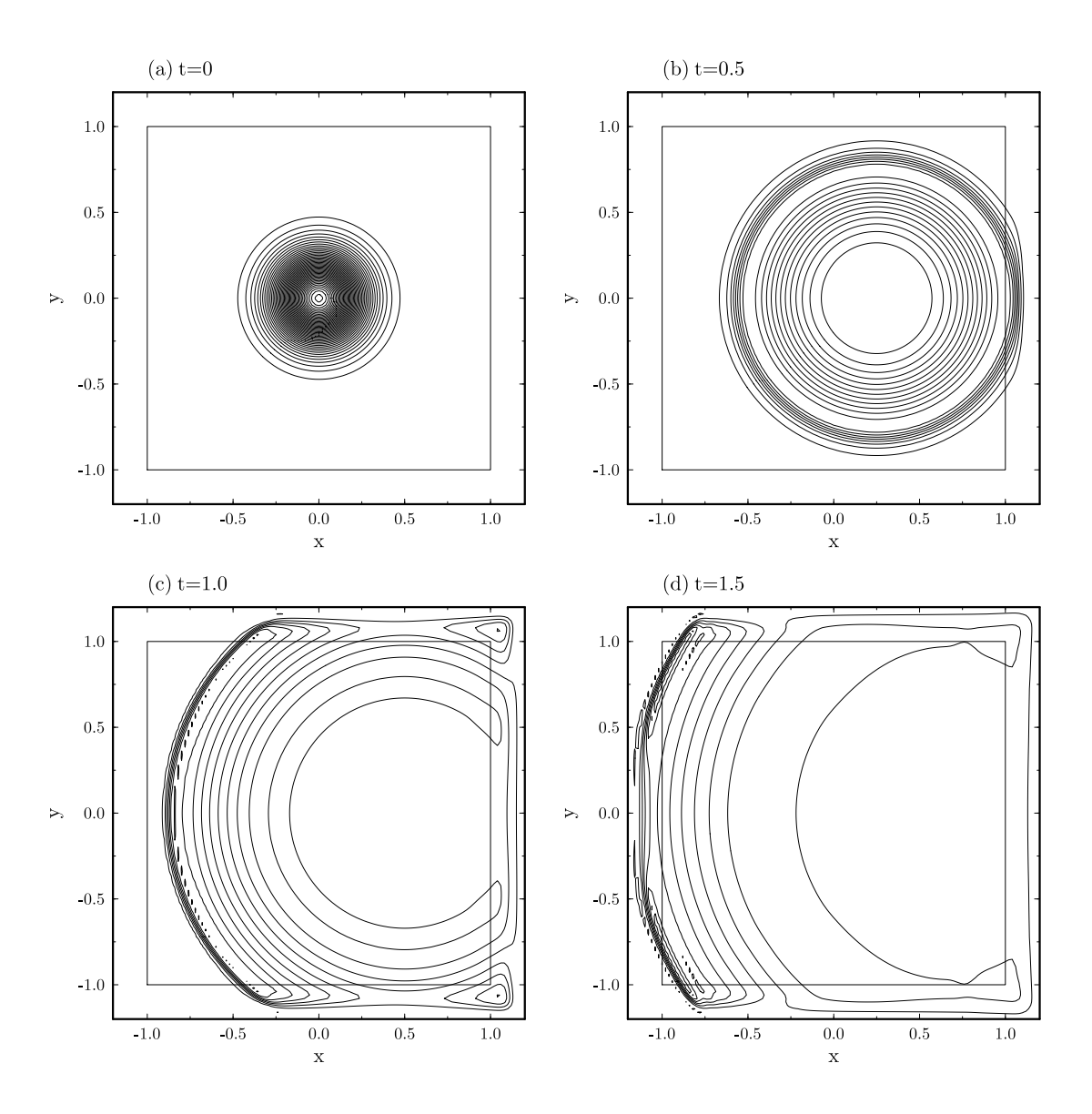


Figure 7. Pressure contours at indicated time.

### C. Absorption of roll-up vortices

In this example, we will simulate the roll-up vortices of a shear flow induced by the Kelvin-Helmholtz instability, and use PML as the absorbing boundary condition as the vortices convect out of the computational domain. The entire computational domain is  $[-1.5, 9.5] \times [-1.1, 1.1]$  with  $\Delta x = 0.05$  and  $\Delta y = 0.01$ , including the surrounding PML domain with a width of 10 grid points. A smaller grid size is used in the y direction in order to better resolve the shear flow. The non-linear Euler equation (1) is solved in the interior physical domain and the PML equations (25)-(26) are solved in the PML domain.

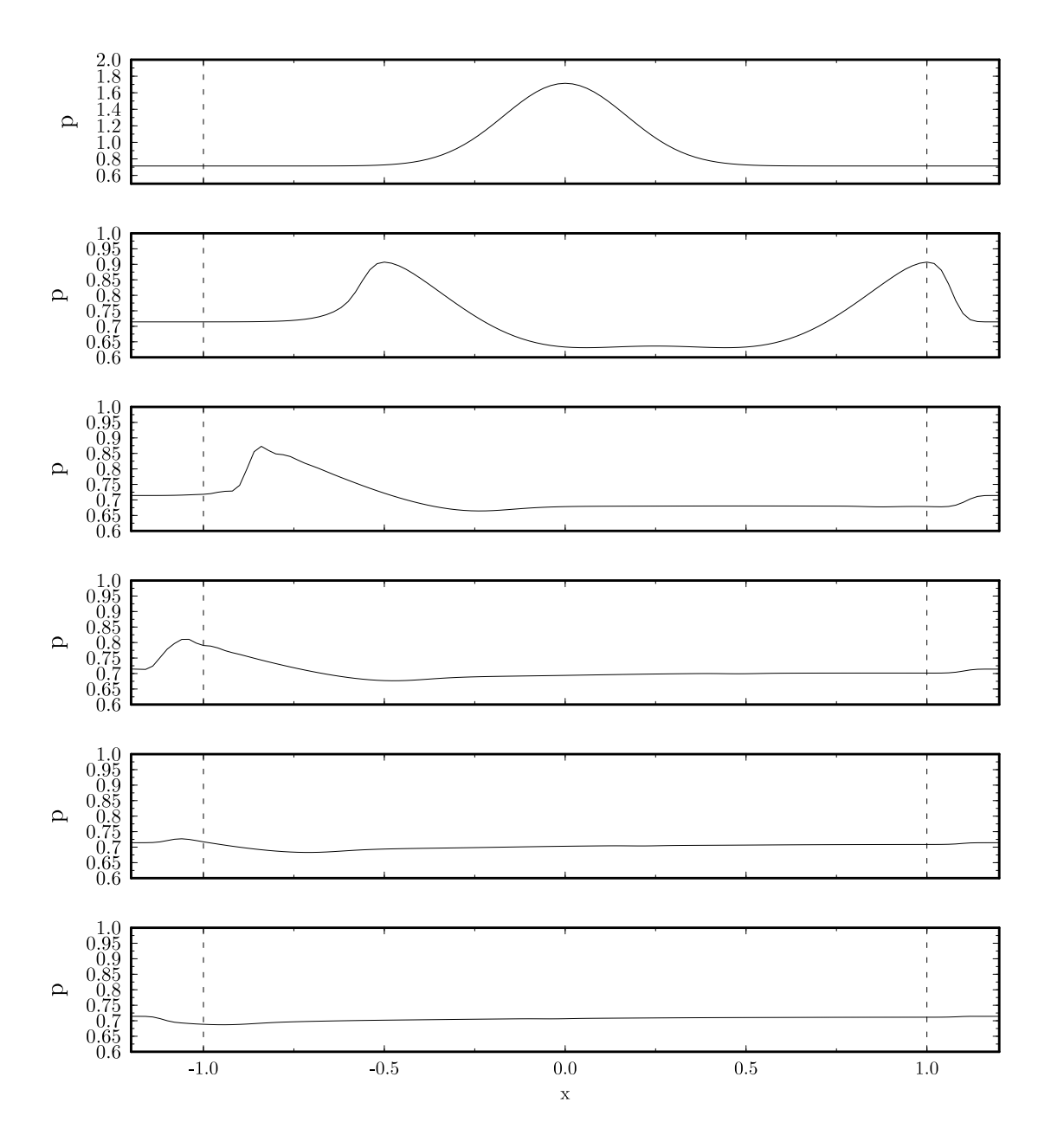


Figure 8. Pressure profile along y=0 at progressive time frames. Vertical dashed lines indicate the Euler/PML interface.

The initial condition in primitive variables is

$$\begin{pmatrix} \rho \\ u \\ v \\ p \end{pmatrix} = \begin{pmatrix} \bar{\rho}(y) \\ \bar{U}(y) \\ 0 \\ \frac{1}{\gamma} \end{pmatrix} \tag{33}$$

where

$$\bar{U}(y) = \frac{1}{2} \left[ (U_1 + U_2) + (U_1 - U_2) \tanh\left(\frac{2y}{\delta}\right) \right]$$
(34)

and

$$\bar{\rho}(y) = \frac{1}{\bar{T}(y)} \tag{35}$$

with

$$\bar{T}(y) = T_1 \frac{\bar{U} - U_2}{U_1 - U_2} + T_2 \frac{U_1 - \bar{U}}{U_1 - U_2} + \frac{\gamma - 1}{2} (U_1 - \bar{U})(\bar{U} - U_2)$$
(36)

where the mean temperature  $\bar{T}(y)$  is determined by the Crocco relation for compressible flows. The parameters are

$$U_1 = 0.8, U_2 = 0.2, \delta = 0.4, T_1 = 1, T_2 = 0.8, \gamma = 1.4.$$

A source term is added to the energy equation in (1) to induce the instability wave. The source term is of the form

$$s(x, y, t) = 5\sin(\omega t)e^{-(\ln 2)[(x-x_0)^2 + (y-y_0)^2]/r_0^2}$$

where  $\omega = \pi/2$ ,  $(x_0, y_0) = (-0.5, 0)$  and  $r_0 = 0.03$ .

The source term will excite the Kelvin-Helmholtz instability wave which will grow exponentially and then develop into roll-up vortices. The vortices at the out-flow boundary, as well as the acoustic waves at the other three artificial boundaries, are to be absorbed by the PML. The pseudo mean-flow  $\bar{\mathbf{u}}_p$  used in the PML equation is the same parallel flow as that of the initial condition (33). The linear wave analysis for this particular shear flow has been carried out in [14], where the value for  $\beta$  was found to be approximately 1/1.4. Figure 8 shows vorticity contours at progressive time frames as the roll-up vortices exit the outflow boundary. As the vortices convect downstream, they are absorbed exponentially in the PML domain. No numerical instability is observed.

In Figure 9, we compare time history of v velocity component at a point close to the outflow boundary with that of a larger domain computation. The numerical solution is given by the solid line and the larger domain calculation by circles. Very little differences were found. This confirms the effectiveness of PML in truncating the outflow in a nonlinear simulation.

It is also possible to use a different pseudo mean-flow at the outflow boundary. In addition to using the initial condition (33) as the pseudo mean-flow in the PML equations, parallel flows of  $\bar{U}(y)$  in the form of (34) with  $\delta = 0.6$  and  $\delta = 0.8$  have also been tested. Figure 10 shows the instantaneous u velocity contours obtained using three different pseudo mean-flow profiles. The results are very similar which implies that all three pseudo mean-flows are viable choices for the PML equations.

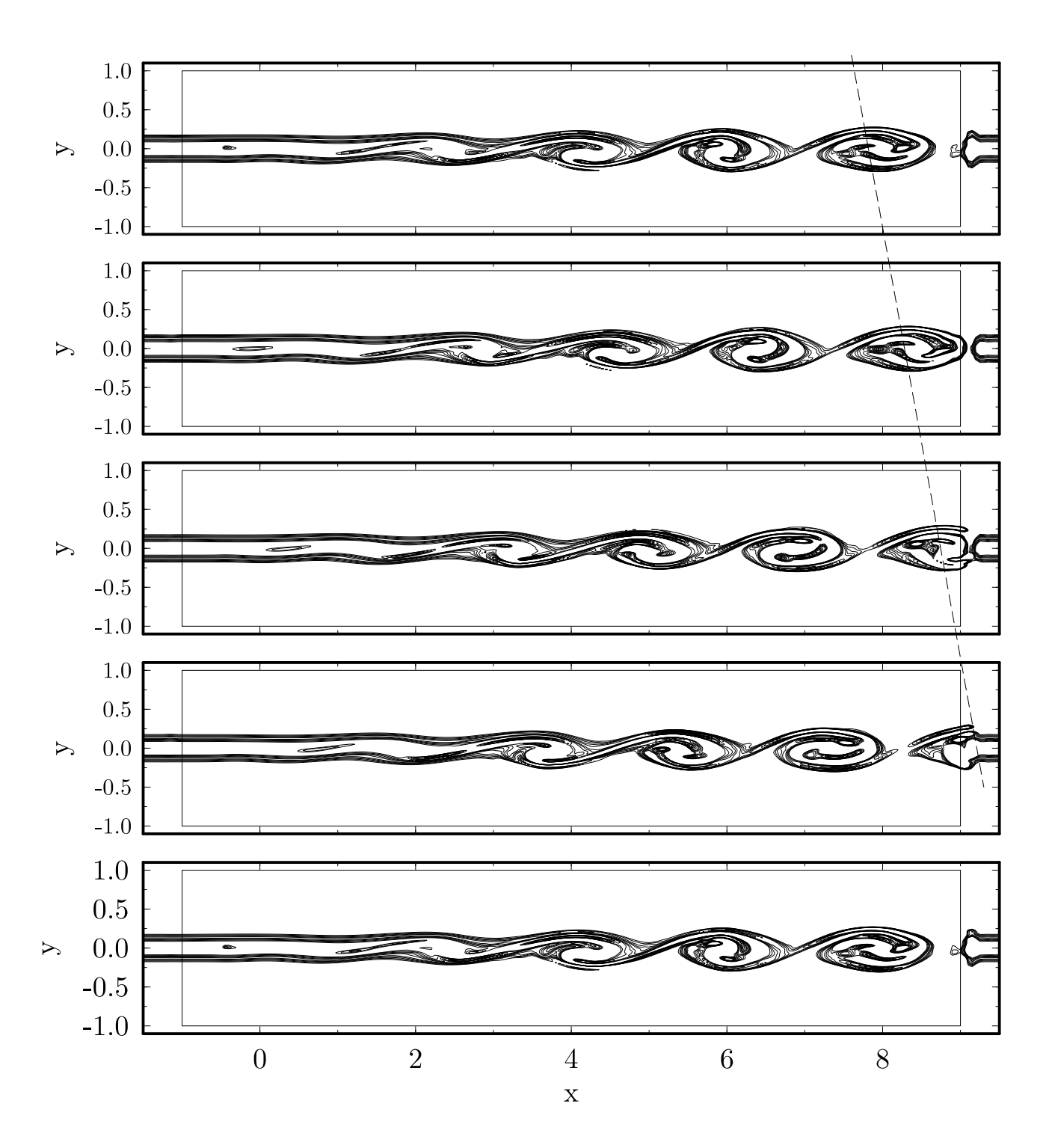


Figure 9. Vorticity contours in progressive time frames.

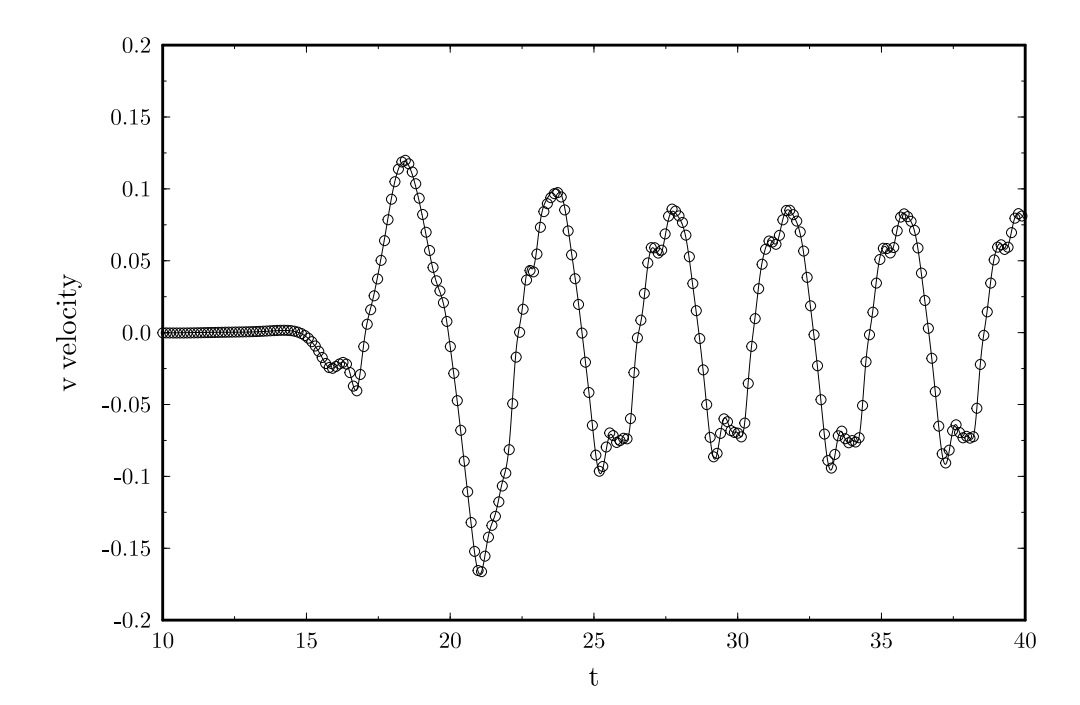


Figure 10. v-velocity as a function of time at a point close to the outflow boundary, (x,y)=(8.75,0.5). Solid line: computational; circle: larger domain calculation.

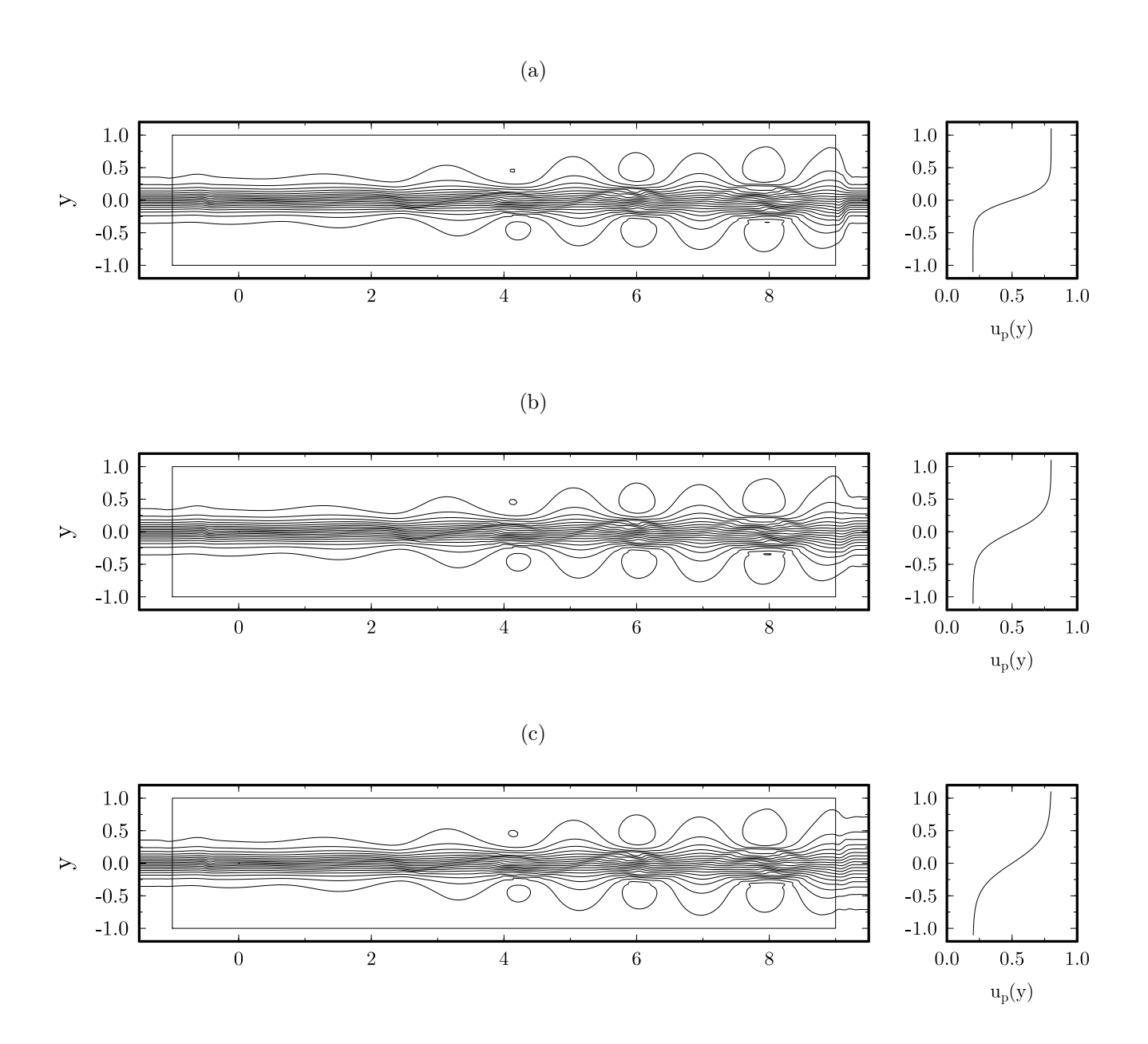


Figure 11. Instantaneous contours of the u velocity and the pseudo mean velocity profile used in the PML equation at the outflow boundary. (a)  $\delta = 0.4$ ; (b)  $\delta = 0.6$ ; (c)  $\delta = 0.8$ .

# V. Conclusions

A time-domain PML for non-linear Euler equation has been derived following recently developed method for linearized Euler equations. By introducing the concept of pseudo mean-flow, the efficiency of PML is increased as it becomes only necessary to absorb the difference between the nonlinear total variable and a prescribed pseudo mean-flow. The pseudo mean-flow is not required to be the same as the exact mean-flow. Considerations on the viable pseudo mean-flows were also presented. Numerical examples of isentropic vortex, nonlinear pressure pulse and roll-up vortices demonstrated the validity and effectiveness of proposed PML as absorbing boundary condition in truncating open boundaries in non-linear Euler simulations.

Since the proposed non-linear PML reduces to the linear PML upon a linearization about the pseudo mean-flow used, the linear stability property of the PML proposed here is the same as that given in [14]. Although no numerical instability has been found in all our computations, theoretical property on the non-linear PML stability remains to be defined.

The success of PML for the fully non-linear Euler equations reported in the present paper is a significant step toward a wider applications of the PML technique for computational fluid dynamics and computational aeroacoustics. The PML presented here can also be extended in a straight forward manner to three dimensional equations and possibly Navier-Stokes equations. Further developments will be reported in future works.

### ACKNOWLEDGEMENT

This work is supported by a grant from the National Science Foundation DMS-0411402.

# References

- <sup>1</sup>E. Becache, S. Fauqueux and P. Joly, Stability of perfectly matched layers, group velocities and anisotropic waves, Journal of Computational Physics, Vol. 188, 399-433, 2003.
- <sup>2</sup>J. P. Berenger, A Perfectly Matched Layer for the Absorption of Electromagnetic waves, Journal of Computational Physics, Vol. 114, 185-200, 1994.
- <sup>3</sup>W. C. Chew, W. H. Weedon, A 3D perfectly matched medium from modified Maxwell's equations with stretched coordinates, IEEE Microwave Opt. Technol. Lett., Vol. 7, 599-604, 1994.
- <sup>4</sup>F. Collino and P. Monk, The perfectly matched layer in curvilinear coordinates, SIAM J. Sci, Comp, Vol. 19, No. 6, P. 2016, 1998.
- <sup>5</sup>S. D. Gedney, An anisotropic perfectly matched layer-absorbing medium for the truncation of FDTD lattices, IEEE Trans. Antennas Propagation, Vol. 44, P. 1630, 1996.
- <sup>6</sup>T. Hagstrom and I. Nazarov, Absorbing layers and radiation boundary conditions for jet flow simulations, AIAA paper 2002-2606, 2002.
- <sup>7</sup>T. Hagstrom and I. Nazarov, Perfectly matched layers and radiation boundary conditions for shear flow calculations, AIAA paper 2003-3298, 2003.
- <sup>8</sup>T. Hagstrom, J. Goodrich, I. Nazarov and C. Dodson, High-order methods and boundary conditions for simulating subsonic flows, AIAA paper 2005-2869, 2005
- <sup>9</sup>M. E. Hayder and H. L. Atkins, Experiences with PML boundary conditions in fluid-flow computations, IUTAM symposium of computational methods for unbounded domains, T. L. Geers (ed.), Kluwer Academic Publishers, 207-216, 1998.
- <sup>10</sup>F. Q. Hu, On absorbing boundary conditions of linearized Euler equations by a perfectly matched layer, Journal of Computational Physics, Vol. 129, 201-219, 1996.
- $^{11}$ F. Q. Hu, On Perfectly Matched Layer as an absorbing boundary condition, AIAA paper 96-1664, 1996
- <sup>12</sup>F. Q. Hu, A stable, Perfectly Matched Layer for linearized Euler equations in unsplit physical variables, Journal of Computational Physics, Vol. 173, 455-480, 2001.
- <sup>13</sup>F. Q. Hu, Absorbing boundary conditions (a review), to appear in International Journal of Computational Fluid Dynamics, 2004.
- <sup>14</sup>F. Q. Hu, A perfectly matched layer absorbing boundary condition for linearized Euler equations with a non-uniform meanflow, Journal of Computational Physics, Vol. 208, 469-492, 2005.
- <sup>15</sup>C. K. W. Tam, L. Auriault and F. Cambulli, Perfectly Matched Layer as an absorbing boundary condition for the linearized Euler equations in open and ducted domains, Journal of Computational Physics, 144, 213-234, 1998.
- <sup>16</sup>E. Turkel and A. Yefet, Absorbing PML boundary layers for wave-like equations, Applied Numerical Mathematics, Vol. 27, 533-557, 1998.
- <sup>17</sup>L. Zhao and A. C. Cangellaris, GT-PML: Generalized theory of Perfectly Matched Layers and its application to the reflectionless truncation of finite-difference time-domain grids, IEEE Trans. Microwave Theory Tech., Vol. 44, 2555-2563, 1996.